Synergies in renewable fuels and exhaust heat thermochemical recovery in low carbon vehicles

Mardani, Moloud; Tsolakis, Athanasios; Nozari, Hadi; Herreros, Martin; Wahbi, Ammar; Sittichompoo, Sak

DOI:
10.1016/j.apenergy.2021.117491

Document Version
Peer reviewed version

Citation for published version (Harvard):
Mardani, M, Tsolakis, A, Nozari, H, Herreros, M, Wahbi, A & Sittichompoo, S 2021, 'Synergies in renewable fuels and exhaust heat thermochemical recovery in low carbon vehicles', *Applied Energy*, vol. 302, 117491. https://doi.org/10.1016/j.apenergy.2021.117491

Synergies in Renewable Fuels and Exhaust Heat Thermochemical Recovery in Low Carbon Vehicles

Moloud Mardani, Athanasios Tsolakis*, Hadi Nozari, Jose Martin Herreros, Ammar Wahbi, Sak Sittichompoo

Mechanical Engineering, School of Engineering, University of Birmingham, Birmingham B15 2TT, UK

Abstract

The impact of renewable fuels on exhaust energy recovery using catalytic thermochemical process in modern gasoline direct injection is studied with main aim of reducing vehicle carbon footprints. It is proven that supplying the engine with increased calorific value reformate would be beneficial in terms of CO_2 reduction and fuel economy. In this research, the influence of butanol and ethanol on heat recovery, H_2 production, and reforming efficiency are analytically and experimentally studied under various key parameters, including steam to carbon molar ratio and reactor inlet temperature under lean engine operating condition. Gibbs free energy and chemical equilibrium analyses are implemented to identify the key reaction pathways in reforming of the fuels. At lower exhaust gas temperatures where the reactions are thermodynamically limited the conversion rate is mainly controlled by the steam to carbon molar ratio and reducing fuel flow rate leads to a significant increase in fuel conversion levels. Maximum calorific value was achieved by ethanol reforming at 600 °C. However, at higher temperatures and steam to carbon molar ratios, butanol generally indicates better performance in terms of engine fuel economy, energy replacement by reformate, and CO_2 reduction. These advantages are attributed to higher calorific value and higher reforming process efficiency of butanol compared to ethanol. In contrast, at lower temperatures, ethanol reforming generates more H_2 as a result of highly endothermic nature of butanol steam and dry reforming reactions compared to ethanol with weaker molecular bonds and higher molecular diffusivity rate which leads to an efficient use of the catalyst.

Keywords: Renewable fuel, Fuel reforming, H_2 production, Gibbs energy minimization method, Thermodynamic analysis, Exhaust energy recovery.

* Corresponding author.
E-mail address: a.tsolakis@bham.ac.uk (A. Tsolakis).

Nomenclature

Symbol	Description and unit
aCat	After Catalyst
bCat	Before Catalyst
CO_2	Carbon dioxide
CO	Carbon monoxide
CZA	Ceria–Zirconia–Alumina
COx	Complete Oxidation
DR	Dry Reforming
EIMS	Electron Impact Ionization Mass Spec
λ	Equivalence Ratio
C_2	Ethane
FTIR	Fourier-Transform Infrared Spectroscopy
GHSV	Gas Hourly Space Velocity [1/h]
GDI	Gasoline Direct Injection
H_2	Hydrogen
IMEP	Indicated Mean Effective Pressure [bar]
LHV	Lower Heating Value [kJ/kg]
Meth I	Methanation I
Meth II	Methanation II
MON	Motor Octane Number
NOx	Nitrogen oxides
O_2	Oxygen
O_2/C	Oxygen to Carbon Molar Ratio
POx	Partial Oxidation
RON	Research Octane Number
Rh	Rhodium
H_2O	Steam
SR	Steam Reforming
S/C	Steam to Carbon Molar Ratio
TWC	Three Way Catalyst
THCs	Total Hydrocarbons
WGS	Water Gas Shift

1 Introduction

The utilisation of renewable fuels has become of great importance as an answer to issues associated to energy security, climate change, environmental pollution and human health effects linked with the use of carbonaceous fossil liquid/solid fuels [1]. The necessity of reducing carbon emissions in road transportation has been reflected in many governmental policy documentations and roadmaps worldwide. This is in line with the global effort to reduce the carbon emissions to meet the global environmental regulations and agreements. With the intention of increasing engine efficiency, waste energy can be thermally recovered and reused [2]. These methods, including Rankine cycle, thermos-

electrics and turbo-charging [3] have been extensively studied and widely developed in recent years. Exhaust thermochemical energy recovery has been achieved by exhaust gas fuel reforming technique [4]. Thermochemical recuperation of liquid biofuels has been studied in recent publications [5],[6],[7],[8],[9]. According to their results, it is feasible to elevate the efficiency of the engine by establishing exhaust gas fuel reforming technique. In this process, exhaust waste energy and combustion products (e.g. CO_2, H_2O, etc.) from engines in presence of fuel injection, can be catalytically utilised to produce a H_2-rich reformate mixture [10].

Previous works have been published reporting the benefits when the reformate products are recirculated to the engine. The engine brake thermal efficiency was improved, while engine out NOx and particle emissios were reduced as a result of exhaust gas diluents and hydrogen addition to the engine intake [11],[12],[13],[14],[15],[16]. Hydrogen's high octane number, absence of carbon, high flame propagation rate, low ignition energy and wide flammability limits can provide stable combustion especially during cold start, fuel economy improvements and reductions in carbon based pollutants such as particulate matter, CO and CO_2 [12],[14]. Furthermore, H_2 in combination with EGR (Exhaust Gas Recirculation) could significantly reduce NOx emissions [15],[16]. Despite the substantial advantages of H_2, widespread applications of H_2 fuelling is prevented because of extant fundamental challenges towards its production, transportation, on-board storage, and safety [15]. For this purpose, considerable research is dedicated to recognise the most appropriate and efficient techniques toward on-board H_2 production including water electrolysis, thermochemical water decomposition [17], biomass gasification [18], and reforming of H_2-containing gas and/or liquid fuels [19].

Exhaust gas fuel reforming has been presented as an effective approach for production of on-board H_2-rich gas using diesel and biodiesel [20], gasoline [21] and ethanol [22] fuels. Implementation of a prototype full-scale exhaust gas fuel reformer coupled with a multi-cylinder GDI engine has been experimentally investigated in different level of reformate at a wide range of engine operating conditions [10],[12],[21],[23]. The experimental results confirm that recirculating the reformate back in the engine (addition of the H_2 and CO to EGR) simultaneously improvement in engine thermal

efficiency, NOx and HCs emissions was achieved [10], with up to 5-6 % improvement in fuel economy and CO_2 reduction [12]. In summary, the integration of a prototype fuel reformer with GDI engine has proven to be applicable, while further study is required to investigate the significant role of fuel composition on fuel reforming efficiency, exhaust heat recovery and engine emissions.

In addition to carbon benefits, ethanol as a non-toxic, sulphur and aromatics free fuel reduces catalyst deactivation rate and surface poisoning and was seen as one of the promising candidates for fuel reforming process [24]. Steam and auto-thermal reforming of pure ethanol were examined experimentally and thermodynamically for different steam to fuel and oxygen to fuel molar ratios, under various range of temperatures and catalysts [22],[25],[26],[27],[28],[29]. Experimental analyses of ethanol steam reforming reveal that steam to carbon ratio has the most significant effect on H_2 production, followed by operating temperature of steam reforming and water gas shift reactions, while liquid flow rate has the least contribution towards controlling the product yield [26]. Minimal catalyst deactivation rate and surface poisoning has positioned ethanol as a feasible candidate for fuel reforming process [24].

In recent years, n-butanol has been applied for fuel reforming applications [30]. Higher heating value and kinematic viscosity, lower risk of vapour lock and cavitation due to lower vapour pressure (volatility) [31] and better inter-solubility quality [32] and resistance against water contamination with respect to ethanol present it as a reliable biofuel.

The majority of studies are focused on butanol steam reforming on fixed bed reactors [33] ,[34],[35],[36],[37],[38] and/or mixed with secondary fuel, mainly gasoline and urea [39]. Detailed thermodynamic analyses of butanol steam reforming have been carried out by Gibbs free energy minimisation method to investigate the optimum operating temperature and steam to carbon molar ratios to attain the most efficient reforming processes and maximum H_2 yield. Steam reforming of butanol ($C_4H_{10}O$) has been also investigated over Ni based catalyst with three different relative atomic percentage of Ni (23, 28 and 33%) in a microscale quartz fixed-bed reactor [38]. Test results revealed

that, increasing inlet temperature favoured fuel conversion and secondary products concentration (CO, CH_4, and C_2). Significant higher operating temperature supressed H_2 and CO_2 production.

Auto-thermal reforming is the combination of steam reforming and the partial oxidation with oxygen of butanol has also been studied using chemical equilibrium calculation [40]. The effect of temperature for auto-thermal reforming of butanol over Rh/ZrO_2 catalyst has been also experimentally studied [34]. For temperatures ranged from 400 °C to 800 °C, the presence of appropriate amount of oxygen during reforming procedure eliminates coke formation while preserving efficiency rate. In overall, an increase in the O_2/C favoured fuel conversion and slowdowns the reforming catalyst deactivation. CO_2, which is one of the most abundant contents in exhaust mixture, can be converted to H_2 rich gas through dry reforming reaction of butanol. This process was investigated thermodynamically as a function of CO_2 to butanol ratio for solid oxide fuel cells (SOFCs) [41]. The results report that the maximum H_2 concentration is achieved in temperatures ranged from 877 °C to 927 °C and for the CO_2 to fuel molar ratios of 3.5 to 4.0.

The effect of operating pressure on reformate composition has been computationally studied in recent years. According to thermodynamic results, the increase of pressure, has a unfavourable effect on the equilibrium and reforming efficiency as a result of change in direction of the reactions. In another word, the main reforming reactions including steam and dry reforming are favoured to proceed in backward direction at high pressure. In this case H_2 and CO productions are suppressed while methane and steam increased. Hence maximum efficiency is achievable at atmospheric pressure [41],[42].

To date, there are no studies that involve the catalytic exhaust gas reforming of butanol as a means of thermochemical waste energy recovery from GDI engines under lean operation. The novelty of this work lies on the analytical and experimental approaches which have been implemented, to investigate H_2-rich reformate production using exhaust from a modern GDI engine. For first time, experiments are focused on GDI lean engine operation, which provides additional engine emissions and fuel economy benefits. This will also facilitate endothermic reactions when exhaust temperature is not high enough,

while preventing coke formation. The most relevant overall reactions are listed in Table 1. The basic parameters including steam to carbon and oxygen to carbon molar ratios, as well as the reactor inlet temperatures were chosen based on realistic engine exhaust conditions. To clarify the key reaction pathways in reforming of the fuels, the method of Gibbs free energy accompanied by chemical equilibrium analyses was implemented. Furthermore, this study investigates the influence of butanol and ethanol biofuels in thermochemical recovery as a way of lowering further the carbon intensity of vehicles. For this purpose, a theoretical method is utilised to estimate CO_2 reduction and energy replacement rate by introducing the reformate in the engine intake. Assumptions are employed in the calculations of those parameters along with identifying the limitations and advantages of each biofuel toward achieving CO_2 emission limit regulations. While the reforming process as a whole is a practical boost to the overall fuel economy and carbon emission of vehicles, the analyses presented here highlight the noticeable impact of operating condition on reforming efficiency, and subsequently, the impact of the process using either of the renewable fuels.

Table 1. General chemical reactions involved in ethanol and butanol reforming process[29],[43],[9],[44].

No.	Reactions	Types of reaction	$\Delta H°_{298k}$ (kJ/mol)
R1	$C_2H_5OH + H_2O \rightarrow 2CO + 4H_2$	Ethanol steam reforming (ESR)	256
	$C_4H_{10}O + 3H_2O \rightarrow 4CO + 8H_2$	Butanol steam reforming (BSR)	558
R2	$C_2H_5OH + CO_2 \rightarrow 3CO + 3H_2$	Ethanol dry reforming (EDR)	297
	$C_4H_{10}O + 3CO_2 \rightarrow 7CO + 5H_2$	Butanol dry reforming (BDR)	681.7
R3	$C_2H_5OH \rightarrow CO + CH_4 + H_2$	Decomposition of ethanol	49
	$C_4H_{10}O \rightarrow C_3H_8 + CO + H_2$	Decomposition of butanol	11.98
	$C_4H_{10}O \rightarrow 2CH_4 + CO + H_2 + C$	Decomposition of butanol	14.19
R4	$CO + H_2O \leftrightarrow CO_2 + H_2$	Water-gas-shift reaction (WGS)	-41
R5	$C_2H_5OH + 3O_2 \rightarrow 2CO2 + 3H_2O$	Oxidation of ethanol (ECOx)	-1366.8
	$C_4H_{10}O + 6O_2 \rightarrow 4CO2 + 5H_2O$	Oxidation of butanol (BCOx)	-2676.8
R6	$2C_2H_5OH + O_2 \rightarrow 4CO + 6H_2$	Partial oxidation of ethanol (EPOx)	43.88
	$2C_4H_{10}O + 3O_2 \rightarrow 8CO + 10H_2$	Partial oxidation of butanol (BPOx)	-115.8
R7	$CO + 3H_2 \rightarrow CH_4 + H_2O$	Methanation reaction I (Meth I)	-206
R8	$CO_2 + 4H_2 \leftrightarrow CH_4 + 2H_2O$	Methanation reaction II (Meth II)	-165
R9	$C_2H_5OH \rightarrow C_2H_4 + H_2O$	Dehydration of ethanol	45
	$C_4H_{10}O \rightarrow C_4H_8 + H_2O$	Dehydration of butanol	-24.04
R10	$C_2H_5OH \rightarrow CH_3CHO + H_2$	Dehydrogenation of ethanol	68
	$C_4H_{10}O \rightarrow C_4H_8O + H_2$	Dehydrogenation of butanol	-86.47

2 Methodology

2.1 Thermodynamic equilibrium analysis

Equilibrium calculations stand on interpolation of the gas-phase chemical reaction mechanism with corresponding thermodynamic properties. In this current study, ANSYS CHEMKIN 18.2 as a highly structured and well stablished software, was utilized to facilitate thermodynamic equilibrium analysis [45]. Zero dimensional simulation serves as a reference to define favourable experimental operating conditions and inlet parameters [46],[47]. Equilibrium method would be particularly beneficial to estimate possibility of the overall reforming process, mechanism reliability, and appropriate operating conditions to reach a reforming system with maximum H_2 production and process efficiency. Furthermore, this technique clarifies reforming process limitations, critical operational temperatures, pressures, and parametric ratios, and provides the possibility of experimental and theoretical comparisons.

In this study, thermodynamic analyses of ethanol and butanol reforming were carried out for both, using exhaust from the lean and stoichiometric engine operation by Gibbs free energy method [29]. The applied mechanism is a combination of the most reliable reforming reactions accredited by several researches and demonstrated acceptable agreement with benchmark experimental results [48],[49].

The mixture composition in the reactor inlet is introduced to CHEMKIN based on the theoretical calculations associated with S/C ratios from 2.0 to 4.0. It is important to note that the calculation of S/C ratio is based on variable fuel injection rate and constant GHSV (Gas Hourly Space Velocity). Catalyst inlet temperature ranged from 400 to 800 °C and inlet pressure was presumed 1.0 bar during the whole analysis. To represent the best experimental operating condition, pressure drop was ignored in all stages and a steady state and isolated system was assumed for equilibrium analysis.

In the last stage, the effects of process variables on reformate composition were monitored to optimise operational temperatures and S/C ratios and to determine the most favourable operating

conditions for ethanol and butanol reforming process. Furthermore, reforming process efficiency was calculated according to theoretical product gas composition of reformate considering simultaneous SR, oxidations, WGS, and DR reactions related to the nominated fuels.

2.2 Experimental procedure and materials

Gasoline Direct Injection (GDI) Engine

All presented experiments in this investigation were performed in 2.0 L, four-cylinder turbocharged gasoline direct injection (GDI) engine, manufactured by Ford, and coupled with a 75kW AC dynamometer to motor and load the engine. Engine specification details are reported in Table *2*. The engine in-cylinder pressure was monitored using an AVL piezo-electric pressure transducer connected to data acquisition system. Indicated mean effective pressure (IMEP) was calculated by using an in house developed LabVIEW software.

Table 2. Engine specifications.

Parameter	
No. of Cylinders	4 cylinders
Displacement	2.0 L
Turbocharger	Borg Warner k03
Compression Ratio	10:1
Bore × Stroke	87.5 × 83.1 mm
Rated Torque	300 Nm at 1750-4500 rpm
Rated Power	149 kW at 6000 rpm
Fuel injection system	Multi-holes, Solenoid actuated, Side mounted
Engine Management	Bosch ME 17

Fuel injection system in the reformer

The fuel injection system in the reformer is composed of a low-pressure fuel pump, fuel injector and mixing chamber. The fuel injector was calibrated based on the fixed fuel volume method at injection pressure of 3.0 bar. The calibration measurements were repeated three times to ensure the repeatability with the maximum standard deviation of 1.06 ms and 3.02 ms for ethanol and butanol, respectively. Fuel injection rate was controlled through microcontroller using pulse-frequency modulation (PFM) technique which utilises fixed turn-on-time and variable frequency. An empirical

derived equation of injection characteristic is obtained using linear equation fitted with $R^2 > 0.99$. The fuels used in this research were ethanol and n-butanol. Fuels properties are indicated in Table 3.

Reforming catalyst

Reforming tests were performed on a Johnson Matthey Ceria–Zirconia–Alumina (CZA) catalyst with coating density of 103.7 kg/m^3 and Rh loading of 2.1 kg/m^3 (1% Rh/CZA). Monolith structure dimensions of the catalyst were 25.4 mm in diameter and 76.2 mm in length, positioned approximately 25.4 cm downstream of the inlet channel and inside a stainless-steel reactor (with diameter and length of 31.8 mm and 127 mm, respectively). The reactor was inserted in tubular furnace, Table 3, which made it possible to monitor and set the reactor temperature.

Table 3. Furnace features.

Model	Carbolite GVA 12/600
Max temp (°C)	1200
Number of heated zones	Single zone
Heated tube length (mm)	600
Heat-up time (mins)	70
Max outer diameter accessory tube (mm)	170
Furnace body length (mm)	780
Max power (W)	3900
Thermocouple type	N

Gaseous species analysers

FTIR (Fourier-transform Infrared Spectroscopy) MKS 2030 multi-gas analyser was used to measure and monitor exhaust gas compositions (including NOx, H_2O, CO, CO_2, CH_4, and THC) both downstream and upstream of the reforming reactor. Sampling mixture was conducted towards FTIR instrument through heated lines and kept at the temperature of approximately 191°C to avoid condensation. H-sense H_2 mass spectrometry operated based on the Electron Impact Ionization Mass Spec (EIMS), was used for continuous measurement of H_2 fraction before and after the reforming reactor. A Testo 340 flue gas analyser was utilised to measure oxygen content before reforming catalyst.

Experimental procedure and fuels

Fuel reforming process depends on parameters including exhaust gas compositions, type of primary fuel, catalyst activity and stability [50]. The output composition of the reforming process is controlled by S/C (steam/carbon) ratio, based on the overall H_2O and carbon present in reformer feed gas [20]. The experiments were carried out in steady-state and lean air-fuel ratio with engine operating condition 35 Nm at 2100 rpm, corresponding to 3.0 bar IMEP. In preparing the engine for tests, coolant and oil temperatures were kept approximately on 95 °C. For all tests, engine was started and warmed up using standard gasoline and the exhaust gas composition and temperature before TWC (three way catalyst) was measured and reported in Table 4. Exhaust flow rate was monitored by Pelton glass tube flow meter, provided the possibility of gas hourly space velocity (GHSV) calculation based on the volumetric flow rate of the exhaust stream and catalyst volume on a constant value of 42000 h^{-1} for all test conditions.

A portion of exhaust flow was derived from a low-pressure (after turbine and before TWC) part of the exhaust system and introduced to mixing chamber, which works as a flow homogenizer where fuel is injected, evaporated and mixed with untreated exhaust gas in order to utilise the exhaust latent heat and facilitate fuel evaporation before interacting with reforming catalyst. Temperature was monitored before and after reforming catalyst simultaneously by using K-type thermocouple.

Table 4. Fuels characteristics [51].

Property	**Values**	
Fuel type	**Ethanol**	**n-Butanol**
Chemical formula	C_2H_5OH	C_4H_9OH
Molecular weight [g/mol]	46.07	74.12
Research octane number [RON]	110	98
Motor octane number [MON]	90	85
Density at 15°C, [kg/m^3]	789	811
Viscosity [mm^2/s] at 40 °C	1.10	2.63
Latent heat of vaporization [kJ/kg]	904	722
Lower Heating Value LHV [kJ/kg]	26.85	33.1
Laminar flame speed [m/s]	63.6	58.5
Auto-ignition temperature [°C]	422.8	385
Adiabatic flame temperature [k]	2195	2340

Catalyst inlet temperature was set on 500, 600 and 700 °C to investigate the effect of exhaust temperature on reformer products and efficiency. S/C ratio from 2.0 to 4.0 could be obtained by

adjusting fuel injection flow rate as shown in Table 5. Based on the target S/C ratio in each condition, exhaust flow rate and fuel injection rate are controlled accurately to monitor the output H_2 level. The reaction pathways and relative composition of the reformer products indicate a correlation between S/C ratios, fuel flow rate and exhaust temperature. To clarify the experimental procedure, the complete schematic of experimental setup is demonstrated in Figure 1.

Table 5. Engine operating condition, exhaust gas composition, and temperature.

Parameter	Value	Unit
Operating condition	35/2100	Nm/rpm
IMEP	3	bar
Exhaust temperature	577	°C
Carbon dioxide (CO_2)	13.79	Vol.%
Carbon monoxide (CO)	3070	ppm
Oxygen (O_2)	1.49	Vol.%
Steam (H_2O)	12.59	Vol.%
Hydrogen (H_2)	684	ppm
Nitrogen oxides (NO_x)	2756	ppm
Total hydrocarbons (THCs)	808	ppm
λ	1.07	

Table 6. Detailed information of reforming tests.

Test No.	Pure Ethanol (mL/h)	Pure Butanol (mL/h)	S/C	Reactor Inlet Temperature (°C)	Exhaust Flow (L/min)
1	47	35	2	500	
2	31	23	3	500	10
3	23	18	4	500	
4	47	35	2	600	
5	31	23	3	600	10
6	23	18	4	600	
7	47	35	2	700	
8	31	23	3	700	10
9	23	18	4	700	

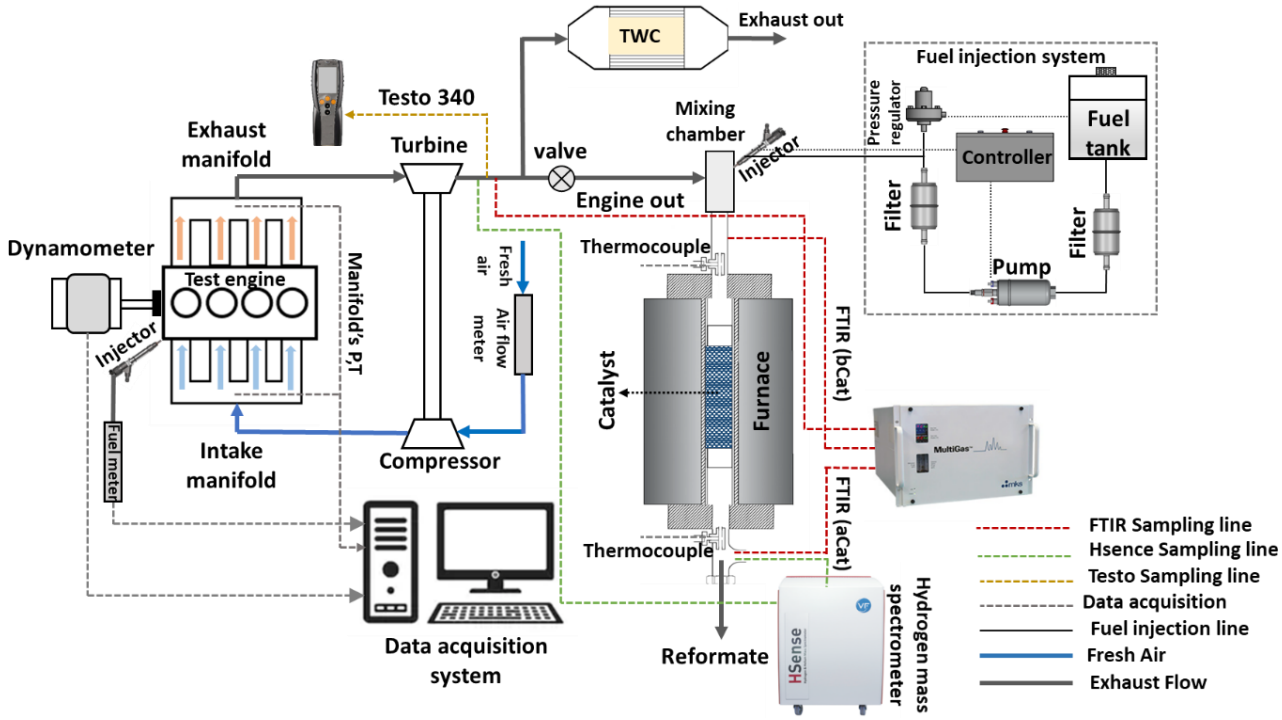

Figure 1. Schematic of experimental setup.

3 Results and discussion

3.1 Thermodynamic analysis of exhaust gas fuel reforming as a function of change in Gibbs free energy

Natural tendency of a reaction always conducts towards achieving the minimum value of ΔG at equilibrium condition, regardless of operating temperature and pressure. The values of Gibbs free energy for the main reforming ethanol and butanol reactions are illustrated in Figure 2.

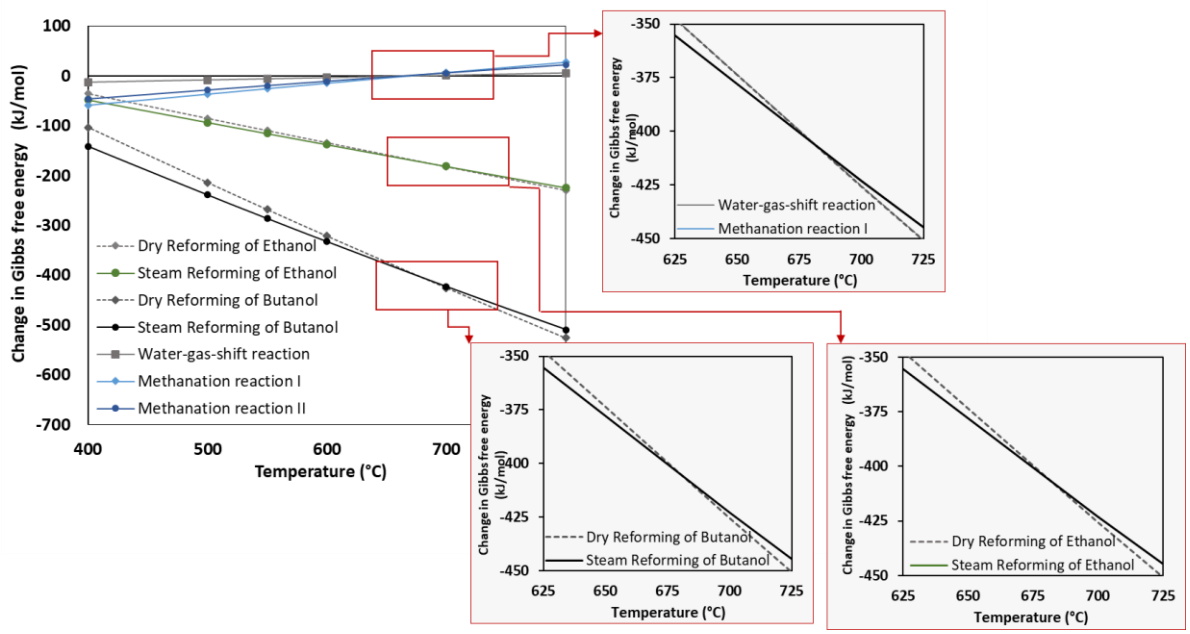

Figure 2. Change in Gibbs free energy of main reforming reactions (listed in Table 1) with respect to the reforming temperature at constant pressure of 1.0 bar.

The same trends were obtained for both fuels, therefore, for clarity in the presentation of the results, only the equilibrium reformate composition results of butanol are illustrated in Figure 3. At low temperature, steam reforming of ethanol and butanol is the most predominant compared to any other participating reactions. It is accompanied with water gas shift reaction, leading to a rapid ascending trend for H_2 production up to about 700 °C. It is also shown how the relationship between H_2 and CO (i.e. H_2/CO) significantly decreases for higher temperatures. This behaviour can be explained based on the Gibbs free energy data shown in Figure 2, indicating that dry reforming of ethanol and butanol is thermodynamically more favourable than steam reforming (T>700 °C). This justifies the relative reduction of H_2 production and H_2O consumption rates as well as an increase of CO production and CO_2 consumption rates for these temperatures. Additionally, by increasing temperature beyond 700 °C, the spontaneity of WGS and methanation reactions decreased gradually to the extent that these reactions became thermodynamically undesirable. As a result, WGS and methanation tend to proceed in reverse direction, resulting in H_2 consumption and methane reforming, respectively.

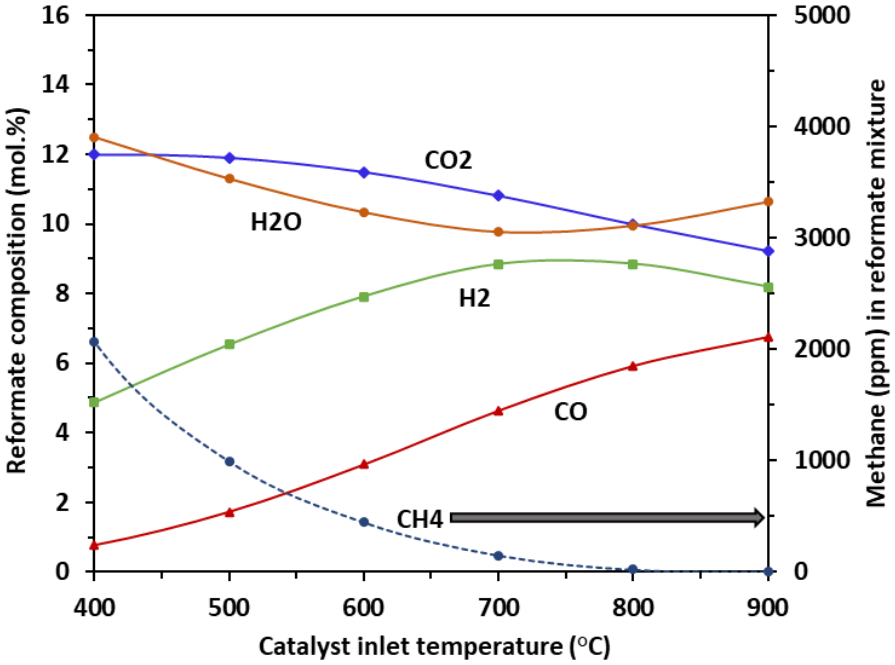

Figure 3. Thermodynamic reformate composition of butanol reforming process as a function of temperature, O_2/C = 0.2 and S/C = 2.0 and fixed absolute pressure 1.0 bar.

3.2 Exhaust gas fuel reforming as a function of temperature, S/C and O_2/C ratio

Butanol reforming using engine exhaust gas from the engine running under lean and stoichiometric operation is evaluated based on equilibrium calculations. The main difference in the exhaust composition is the higher oxygen concentration (and thus the O_2/C ratio) when the engine running in lean conditions. Exhaust flow rate is maintained constant for both exhaust conditions (lean and stoichiometric), hence increasing the fuel injection quantity leads to a lower S/C ratio. The results are shown in Figure 4 (a)-(e), for temperatures ranging from 400 °C to 900 °C, fixed pressure of 1.0 bar and reformer S/C ratios from 2.0 to 4.0. For stoichiometric condition, the trends are in agreement with [42].

The effects of S/C and O_2/C ratio are more noticeable at high temperature, where the reaction are not thermodnamicly limited, especially in the case of exhaust reforming from lean engine operation. In this case (lean exhaust), the maximum H_2 production shifts towards lower temperature for higher S/C ratios. In addition, H_2 content in the reformate is adversely affected at high temperatures. At constant S/C ratio, engine operation (quantified by O_2/C) has a substantial influence on H_2 production. At low temperature, the oxygen content in exhaust mixture derived from lean engine operation leads to

higher H_2 yield in reformate compared to stoichiometric condition. The oxygen presence promotes exothermic reactions and increases heat generation rate. Therefore, as a conscience endothermic reactions (steam and dry reforming) are promoted leading to higher H_2 production. However, at high temperature, the effect of O_2/C is suppressed by temperature, since latent heat of exhaust will be enough to initiate endothermic reactions.

CO is mostly generated by dry reforming of fuel. CO formation trend is very similar to H_2 production at low operation temperatures for all the S/C ratios. However at higher temperature, CO production is enhanced by temperature, particularly in the reforming fuel rich condition (S/C = 2.0). Methane level in reformate mixture declines sharply with temperature as illustrated in Figure 4 (e). This can be explained based on the unspontaneous nature of methanation reactions ($\Delta G > 0$) at high operating temperatures (Figure 2) which leads to methane reformation rather than methane production. This effect is more intense when oxygen is present in the mixture [52].

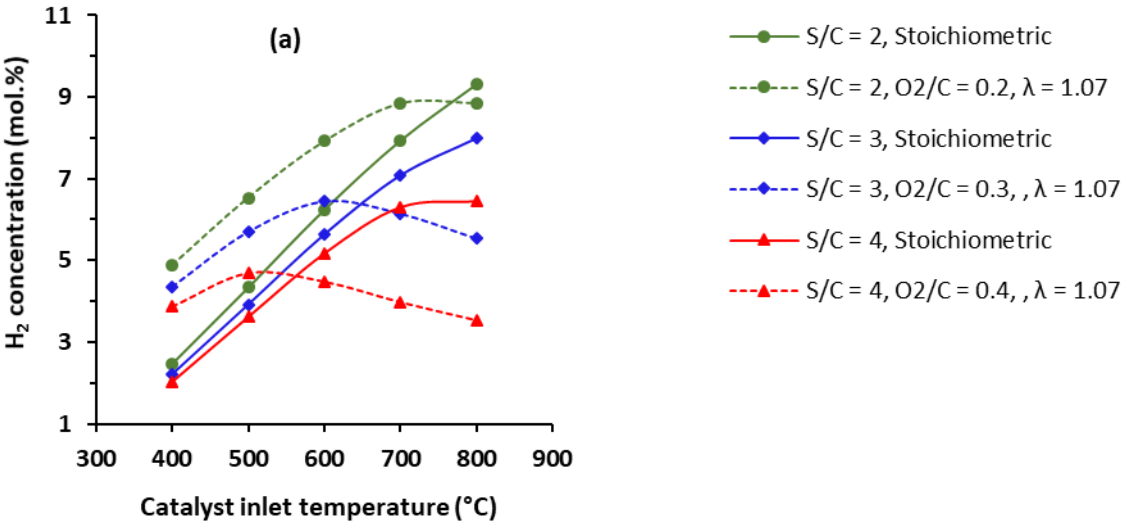

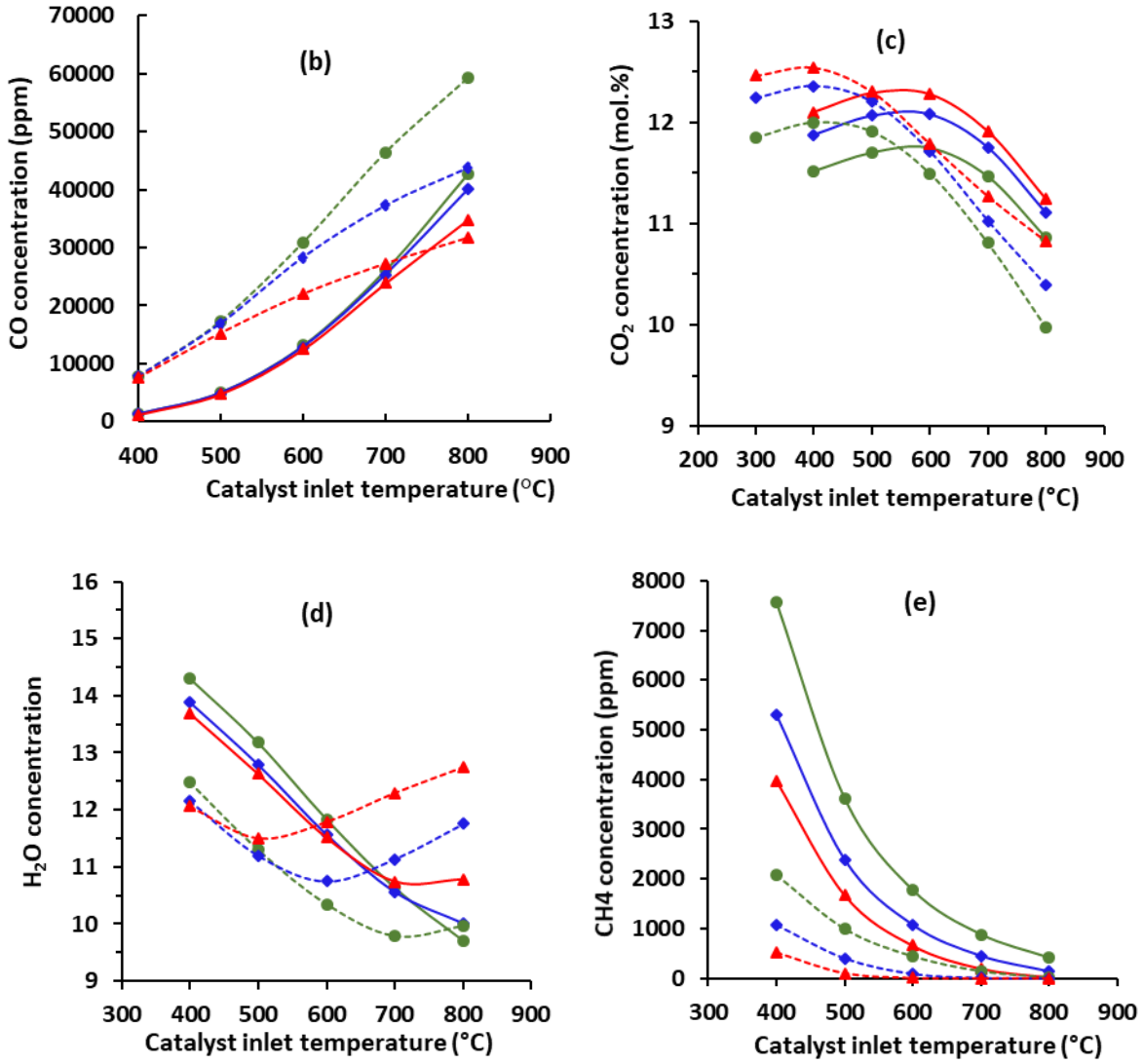

Figure 4. Equilibrium reformate composition as a function of temperature, S/C, and O_2/C ratio. (a) H_2 mol. %, (b) CO (ppm), (c) CO_2 mol. % (d) steam mol. %, (e) methane ppm. Butanol is considered as reformed fuel.

3.3 Experimental analysis of H_2 and H_2O exhaust gas fuel reformate composition

Figure 5 (a) evaluates the performance of butanol reforming process. Both experimental and equilibrium data indicate that H_2 yield is favoured by increased (uo to a point) fuel injection rate (S/C ratio). Since there is heat available increased fuel promotes further the endothermic reactions particularly steam and dry reforming. Similar trends are observed in Figure 5 (b) for the H_2 production during the ethanol reforming process.

Thermodynamic analysis of butanol steam reforming shows similar H_2 production [30] to ethanol reforming. However, the experimental results shown in Figure 5 (a) and (b) reveal that the H_2

production from ethanol reforming is generally higher than butanol. This can be explained by highly endothermic nature of butanol steam and dry reforming reactions (R1 and R2 in Table 1) in comparison with ethanol reforming process. At constant temperature, higher molecular diffusivity and weaker molecular bonds of ethanol increase the chance of reaching the active site of the catalyst and promote the reforming reactions.

Formation of carbon and consequently catalyst deactivation during the reforming process is an essential subject which can impact the catalyst performance. Both equilibrium and experimental analyses were performed by [40],[46],[53],[54],[55] on the reforming of pure ethanol and butanol in the wide range of temperatures and steam to carbon molar ratios. The results revealed that carbon formation can be insignificant under presented steam and O_2 additions.

Experimental and equilibrium values, depicted in Figure 5 (b), show that H_2 production increased to a point, followed by a gradual reduction with simulantius increase in CO as s described later on in Figure 8. The trends can be explained according to the reaction sequences occurring in reforming process, shown in Figure 2. At lower catalyst inlet temperatures, steam (R1) and water gas shift reaction (R4) are responsible for the the H_2 production. Based on the Gibbs free energy graph (Figure 2) steam reforming is less endothermic than dry reforming which makes it the main reaction towards H_2 production at lower inlet temperatures [22]. After achieving the maximum H_2 yield reforming reaction rates reduced smoothly. This is due mainly to the further increase in inlet temperature after reaching maximum H_2 production, that promotes dry reforming over steam reforming [22]. Furthermore, high temperature operating condition suppresses water gas shift reaction and shifts it towards reverse direction, which results in H_2 consumption. As it is illustrated in Figure 5 (b) for ethanol, the experimental maximum H_2 yields are obtained between 650 °C and 700 °C. However, based on the experimental trends shown in Figure 5 (a) for butanol, maximum H_2 yields are not attained until 700 °C, being expected to be achieved at higher catalyst inlet temperature than those predicted by equilibrium [38].

Increasing S/C ratio promotes steam reforming and WGS reactions. According to Figure 2 and Gibbs energy assessment, these reactions are more dominant in lower operating temperatures. Comparison between equilibrium and experimental results in Figure 5 (b), shows that the H_2 production from the experiments are generally higher than H_2 production from the equilibrium analysis. It can be concluded that the reactor (i.e. monolith catalyst) structure has a substantial effect due to continuously changing temperature and reactants along its length. Effect of insufficient catalyst residence time on reformate composition is another potential factor responsible for differences between experimental results and chemical kinetics predictions. Based on Figure 5 (a), in some cases, experimental results illustrate lower H_2 produced than the results from equilibrium counterparts.

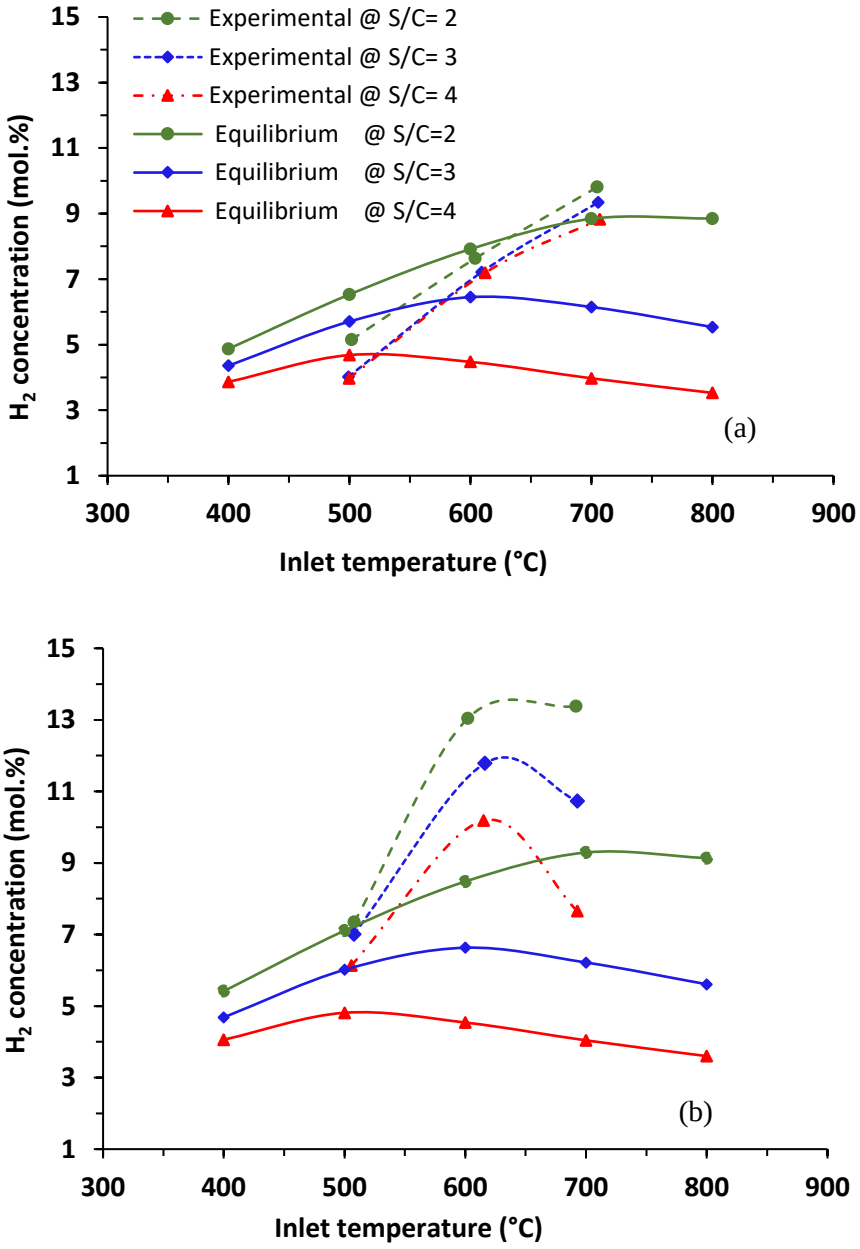

Figure 5. Equilibrium and experimental H_2 production as a function of temperature for reforming of (a) butanol, and (b) ethanol for three different S/C ratios.

Water gas shift, as a fundamental reaction in fuel reforming reactor, converts CO to H_2 through an exothermic process (Table 1). As it is shown by equilibrium trends in Figure 6 (a) and (b), at lower catalyst inlet temperature H_2O concentration in reformate mixture decreased with temperature. Equilibrium trends reveal that water gas shift reaction is thermodynamically limited at high temperature operating conditions [22],[27], as a result of Gibbs free energy increment with

temperature (Figure 2). Thereby, WGS reaction shifts towards reverse direction, which results in H_2 consumption rather than CO conversion and H_2 production.

A comparison between Figure 6 (a) and (b) reveals that the steam concentration at the reformate products from butanol reforming is higher than the values measured for ethanol reforming process. This can be explained based on the feasibility of ethanol steam reforming at lower operating temperatures in comparison with butanol, as well as lower endothermic strength of ethanol steam reforming. As a result, favourability of ethanol steam reforming leads to higher steam consumption and accordingly lower steam concentrations in reformate mixture. Furthermore, a comparison between the graphs in Figure 6 indicates that for ethanol, H_2O fraction will be minimised at lower inlet temperature, approximately between 625 °C to 650 °C. However, as it is estimated by equilibrium and experimental results water concentration will reach its minimum value at higher catalyst inlet temperatures for butanol fuel reforming.

In general, equilibrium predicted higher water reformate concentration compared to experimental measurements for both fuels, particularly at high catalyst inlet temperature. This proves that catalyst has substantial contribution in H_2 production via steam reforming as well as a non-substantial contribution of the water gas shift reaction [22] due to rapid thermodynamic inhibition for water gas shift reaction [34].

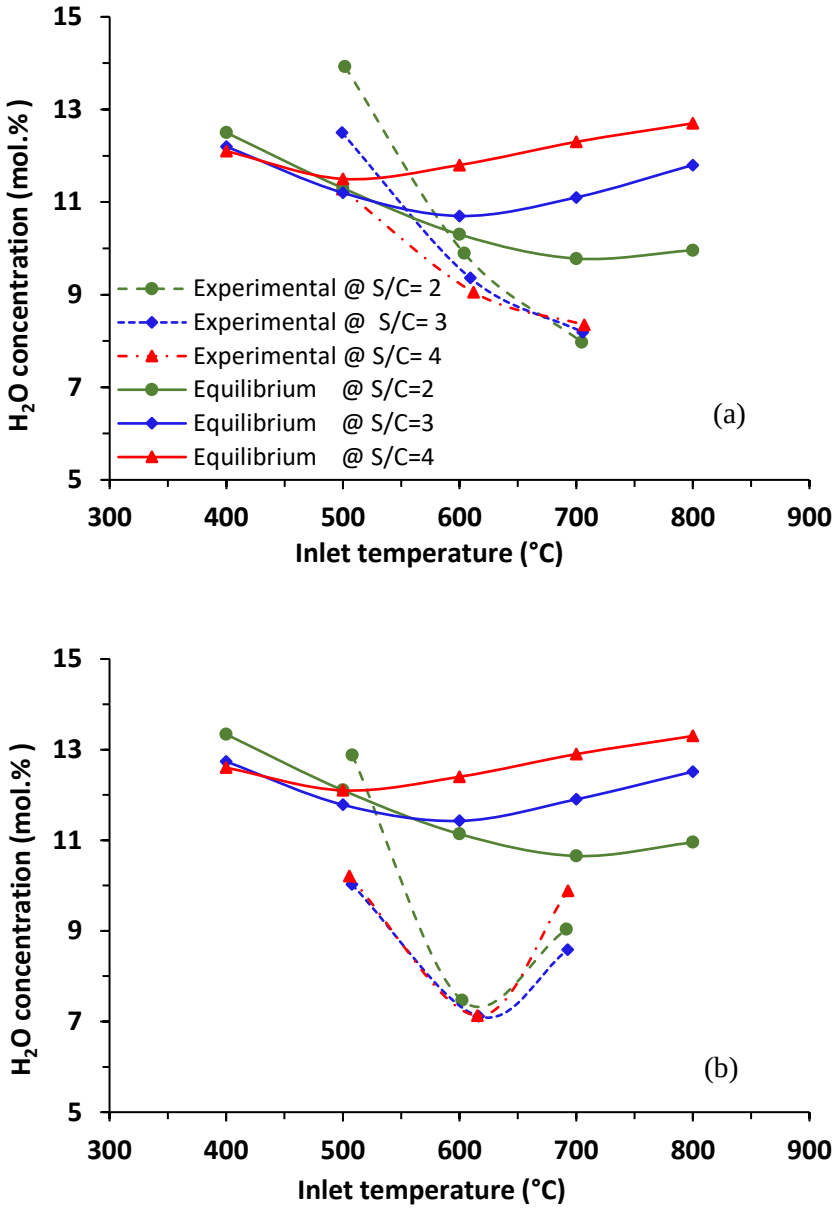

Figure 6. Equilibrium and experimental H_2O production as a function of temperature for reforming of (a) butanol, and (b) ethanol for three different S/C ratios.

3.4 CO_2 and CO trends in the reformate composition

CO_2 concentration as a function of temperature and steam to carbon feed ratio is depicted in Figure 7. It is evident that experimental trends are in acceptable agreement with equilibrium results. Referring to Figure 7 (a) and (b), by enhancing steam to carbon molar ratio CO_2 content in mixture increased accordingly, since more fuel injection resulted in more oxidation reactions and CO_2 production. Furthermore, CO_2 concentration in reformate mixture declined sharply by temperature increment from 500 °C to 700 °C and steam to carbon feed ratio of 2.0 (fuel rich) to 4.0 (fuel lean).

Detailed analysis of both equilibrium and experimental curves revealed that CO_2 consumption rates at temperatures roughly higher than 600 °C are higher than those for temperatures lower than 600 °C. This reforming performance can be explained based on reaction sequences through the reforming process. As indicated in Figure 2, dry reforming as a high endothermic reaction, is more favourable in higher operating temperatures. Correspondingly, after 600 °C, R_2 together with the reverse water gas shift reaction (R_4) consume greater proportion of available CO_2 content in exhaust mixture, which leads to further CO_2 reduction.

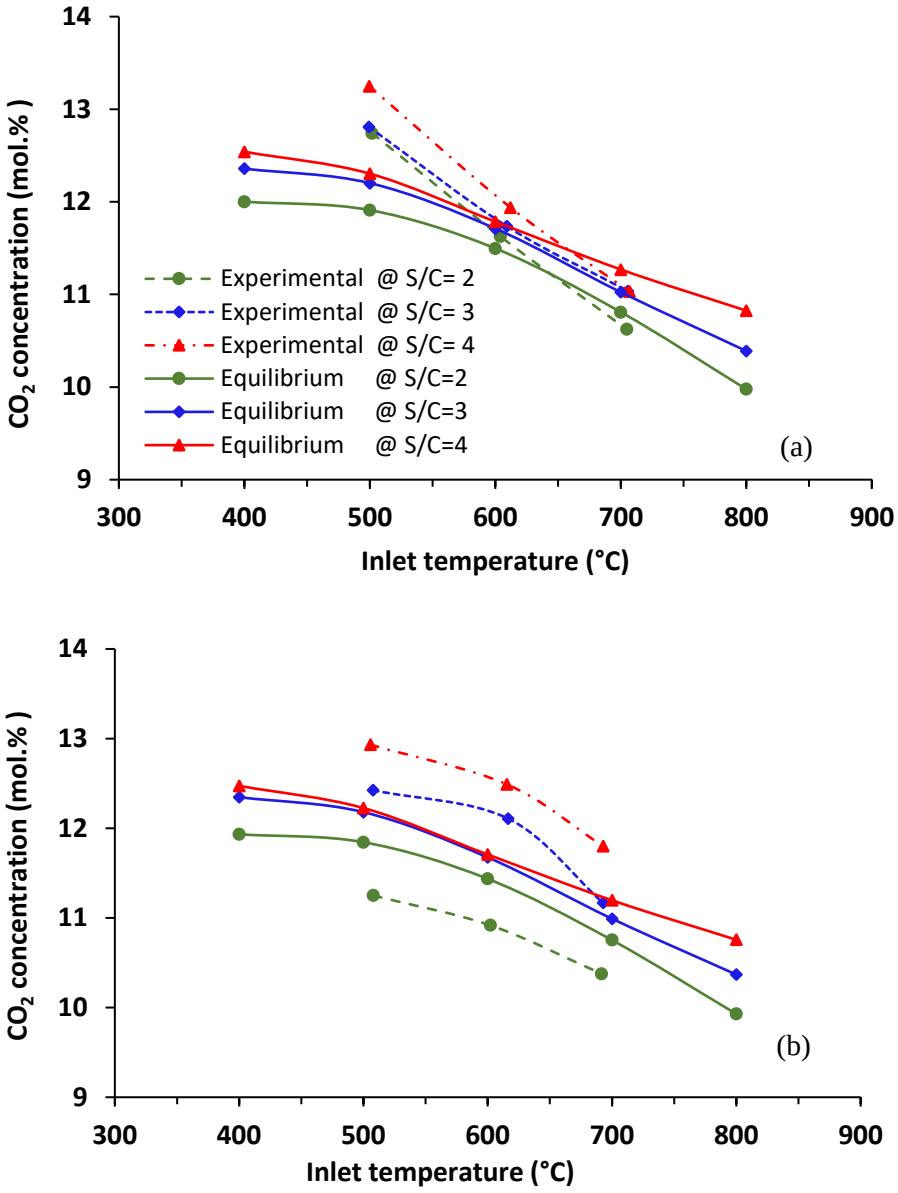

Figure 7. Equilibrium and experimental CO_2 production as a function of temperature for reforming of (a) butanol, and (b) ethanol for three different S/C ratios.

Competition between steam and dry reforming determines CO production level for all inlet temperatures. Trends are depicted based on experimental results and thermodynamic equilibrium predictions in Figure 8 (a) and (b). Temperature increment favours CO production, as firstly CO concentration is enhanced gradually followed by a relatively sharp increase. This trend is more visible in butanol curves shown in Figure 8 (a). Considering Figure 2, at lower catalyst inlet temperatures (approximately at 700 °C) steam reforming is more prominent than dry reforming. However, at higher temperatures, dry reforming as well as reverse water gas shift and methanation facilitate CO

production. Figure 8 (a) shows that at temperatures from 500 °C to 600 °C, CO is mostly produced by gas phase reactions as experimental curves are very similar to equilibrium predictions. However, at higher temperatures , temperature increment benefits CO production by increasing the contribution of surface reactions. Figure 8 (a) and (b) also reveals that higher steam to carbon ratio suppresses CO production rate due to the stronger role of water gas shift reaction towards CO consumption, which agrees with the study by Wang et al. [56].

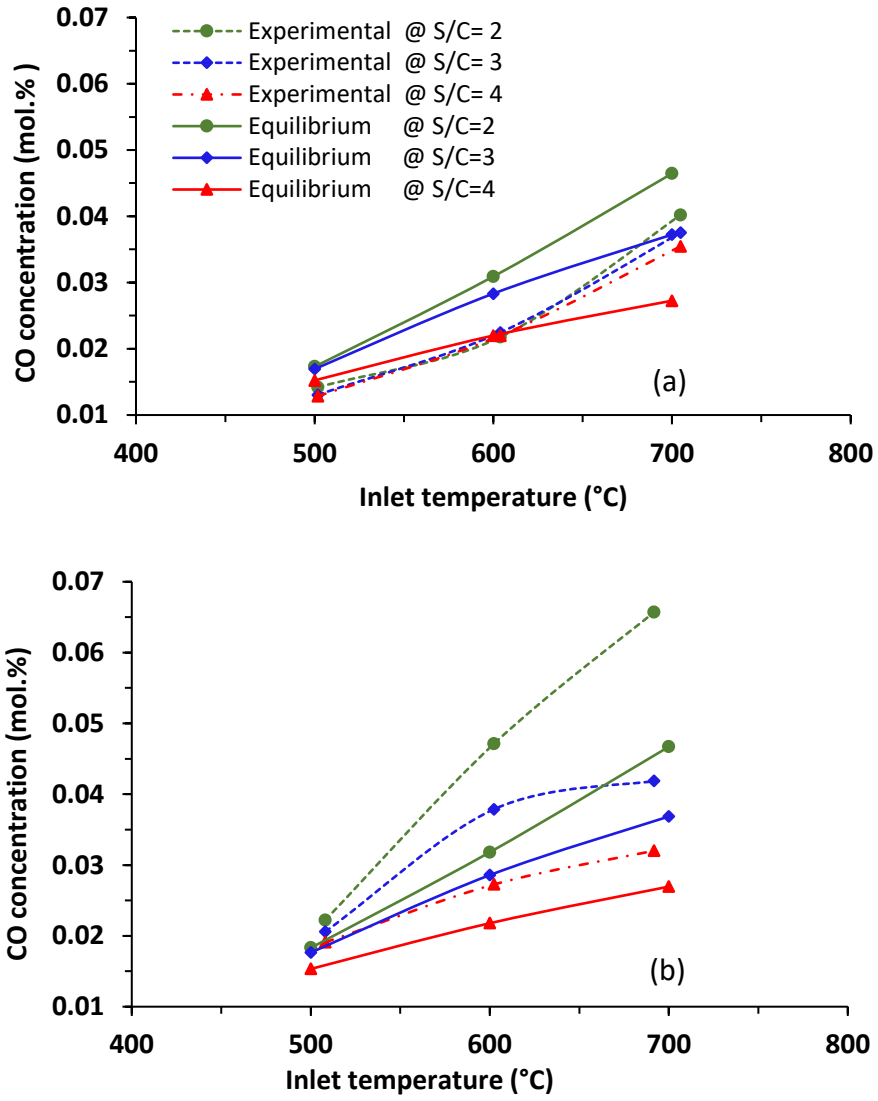

Figure 8. Equilibrium and experimental CO production as a function of temperature for reforming of (a) butanol, and (b) ethanol for three different S/C ratios.

3.5 Fuel conversion and exhaust gas fuel reforming process efficiencies

The fuel conversion rate, illustrated in Figure 9, is calculated based on the Equation 1. Conversion trends prove that temperature increment favours higher fuel conversion rate. This behaviour can be explained based on the better probability of endothermic reactions, including steam and dry reforming, occurring at higher inlet temperature which leads to a greater fuel reforming rate.

$$\text{Fuel Conversion } (\%) = \left(\frac{\text{moles of inlet fuel } - \text{ remained fuel in outlet}}{\text{moles of inlet fuel}}\right) * 100 \quad (1)$$

Equilibrium calculations predict complete fuel conversion for all temperatures and S/C ratios. Comparison between the experimental conversion rates at 600 °C and 700 °C reveals that at lower catalyst inlet temperature, increasing S/C ratio (by reducing fuel flow rate) leads to a significant increase in fuel conversion rate, the same trend as Leung et al. [22], from 33.8% to 77.0% for ethanol and from 42.9% to 73.7% for butanol. However, at higher temperature, conversion rates moderately increase from 82.2% to 99.95% for ethanol and from 73.3% to 93.2% for butanol. It can be concluded that at very high operating temperature, the effect of temperature becomes more dominant and fuel conversion will be independent from S/C ratio. Hence complete fuel conversion is expected at high operating temperatures, as it is predicted by equilibrium results.

Fuel flow rate and competition on similar active site of catalyst affect fuel conversion rate. This effect is more visible at lower S/C ratio, while in higher S/C ratio conversion rates are closer to each other approaching to a negligible difference even at higher temperatures.

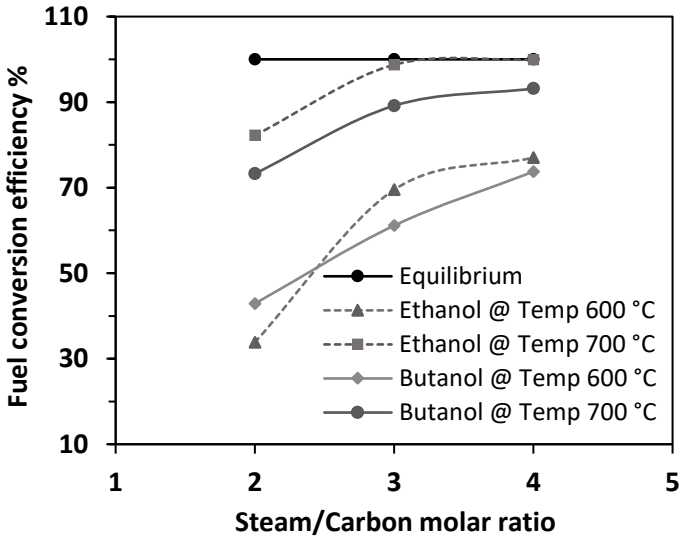

Figure 9. Ethanol and butanol conversion efficiency as a function of temperature and steam to carbon molar ratio.

Reforming efficiency is calculated using Equation 2, shown in Figure 10 and Figure 11, as a function of inlet temperatures and feed steam to carbon ratios, considering thermodynamic and experimental reformate compositions, respectively. LHV $_{\text{fuel prod}}$ and LHV $_{\text{fuel in}}$ refer to lower heating value of CO and H_2 at reactor outlet and fuel (ethanol and butanol) at reactor inlet, respectively [40]. It has to be noted that hydrocarbon species and unconverted fuel have not been taken into account in the efficiency calculation. However, those species would be utilised when the reformate is fed to the engine, increasing the overall process efficiency.

It is worth mentioning that reforming efficiency in this context is the ratio between the output energy of reformate to the input energy of input fuel which heat energy input for reforming is considered as 'free energy'. As for the energy fraction in combustible gas species in the initial exhaust gas (e.g. CO, THCs, and H_2) are insignificant compared with energy from reforming fuel (input fuel), hence, they are negligible in the calculation. Thus, it is possible for 'reforming efficiency' in this context to be greater than 100% which indicates that the whole reforming process is endothermic and heat is recovered and used for the reforming process [21],[57].

$$\text{Reforming efficiency }_{H_2\&CO}\,(\%) = \frac{\text{LHV}_{\text{fuel prod}}\,\dot{m}_{\text{fuel prod}}}{\text{LHV}_{\text{fuel in}}\,\dot{m}_{\text{fuel in}}} \times 100 \qquad (2)$$

Thermodynamic analysis was implemented to investigate oxygen to carbon ratio and temperature influence on theoretical reforming efficiency, as shown in Figure 10. The results has reasonable consistency with the equilibrium results reported by Horng et al [40].

At constant operating temperature, competition between fuel conversion by oxidation reactions and reforming reactions, determines reforming efficiencies. At low inlet temperature, i.e. 500 °C, increase in S/C ratio favours reforming efficiency, while at higher operating temperatures efficiency reaches to its maximum value at S/C = 3.0 (O_2/C= 0.3) and drops gradually in S/C = 4.0 (O_2/C= 0.3). Efficiency trends for stoichiometric engine operating conditions (O_2/C = 0, S/C = 2.0 - 4.0) are different, showing proportional relationship with both temperature and S/C ratios. Based on Figure 4 (c), reduction of CO_2 by temperature increment, leads to continuous production of H_2 and CO and subsequent enhancement of efficiency. In this case, the maximum reforming efficiency is predicted at 700 °C for S/C = 4.0 under stoichiometric exhaust mixture.

Reforming efficiency, calculated using the experimental results, is presented in Figure 11 (a) and (b). In both cases, the efficiency increases with temperature and steam to carbon ratio, with a substantial increase to its maximum level for S/C = 4.0 at 700 °C and 600 °C for butanol and ethanol, respectively. The trends are identical with H_2 production graphs shown in Figure 5 (a) and (b). As H_2 production was increased with temperature during butanol reforming, the same competition was observed for ethanol reforming, as for S/C = 3.0 and 4.0, efficiency and H_2 rate increased considerably to the peak point at temperature 600 °C and then followed by a gentle decrement at 700 °C. To quantify, contribution of only the H_2 content in efficiency value is calculated by Equation 3 and shown in Figure 11, (a) and (b). Contribution of H_2 in efficiency values is greater at lower temperatures (500 °C).

$$\text{Reforming efficiency}_{H_2}\,(\%) = \frac{\text{LHV}_{\text{H2}}\,\dot{m}_{\text{H2}}}{\text{LHV}_{\text{fuel in}}\,\dot{m}_{\text{fuel in}}} \times 100 \qquad (3)$$

In terms of feed S/C ratio, increasing S/C ratio enhances reforming efficiency, taking into account both CO and H_2. The reason is higher S/C ratio for the same amount of oxygen content in the exhaust mixture increases the temperature and recovers the waste heat utilised for fuel vaporisation.

Unreacted hydrocarbon species present in reformate mixture also incorporate positive contribution in reforming efficiency as well as reformate enthalpy since they are combustible and include considerable amount of chemical energy.

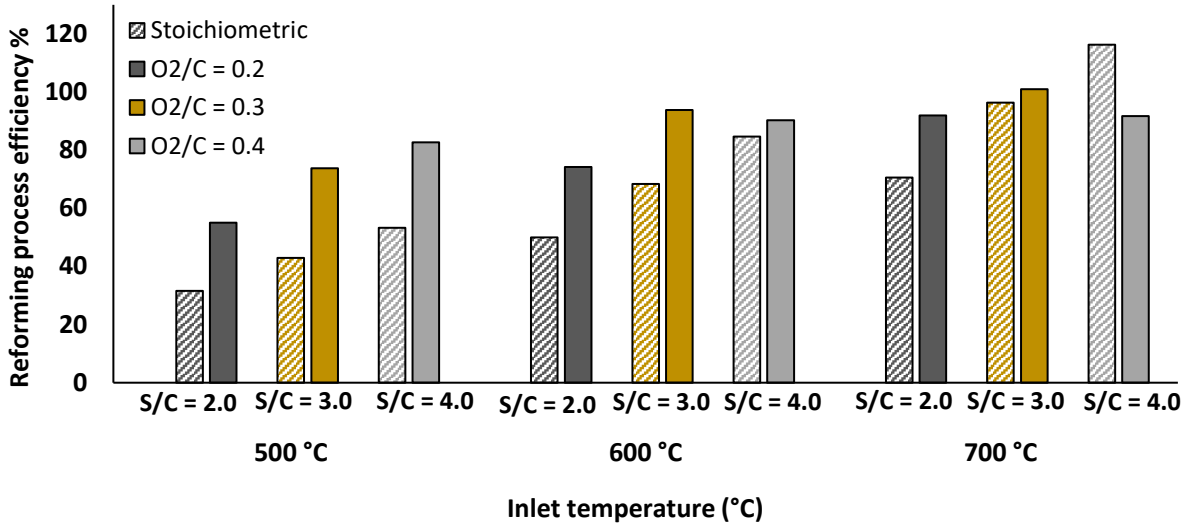

Figure 10. Thermodynamic process efficiency under lean and stoichiometric engine operating conditions for butanol fuel reforming process.

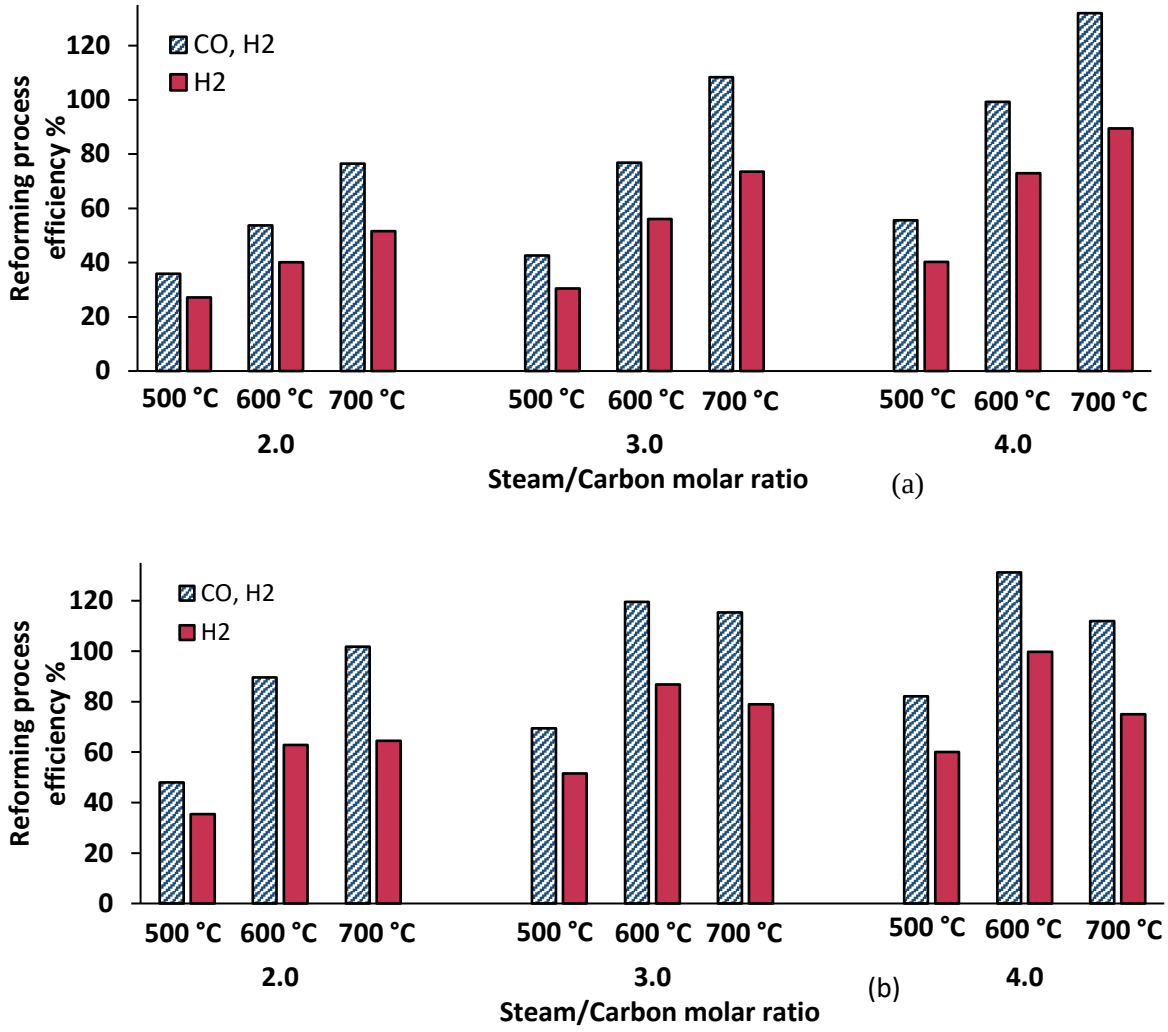

Figure 11. Reforming process efficiency under lean engine operating condition, as a function of steam/carbon molar ratio and temperature for (a) butanol and (b) ethanol.

3.6 CO_2 reduction, incresed calorific value and energy replacement

Figure 12 compares the CO_2 reduction levels for different S/C ratios and reforming temperatures, using ethanol and butanol as reforming fuels. The results confirm that reforming technique is beneficial in terms of CO_2 reduction for both fuels. With regard to the sensitivity of fuel injection rate and operating temperature on CO_2 reduction, it is clear that increasing the steam to carbon ratio and temperature can diminish CO_2 emission. A reason for this reduction is that the presence of H_2 and CO in reformate positively affects combustion efficiency and proportionally decreases overall fuel consumption value and thus CO_2 formation. This benefit is more significant for ethanol in particular at 600 °C where the maximum H_2 production can be achieved, as shown in Figure 5. Therefore, the best overall reduction

of 11.4% is obtained by ethanol at 600 °C and steam to carbon ratio of 2.0. At higher operating temperature butanol reforming leads to about 27.3% greater CO_2 emission reduction as a result of reformate quality improvement. This trend is very similar to the efficiency graph, Figure 11(a), where higher reforming process efficiency was gained by butanol reforming at temperature 700 °C. Overall, the advantage of ethanol reforming on CO_2 formation is greatest at lower temperature while butanol can yield an additional CO_2 reduction at higher temperature.

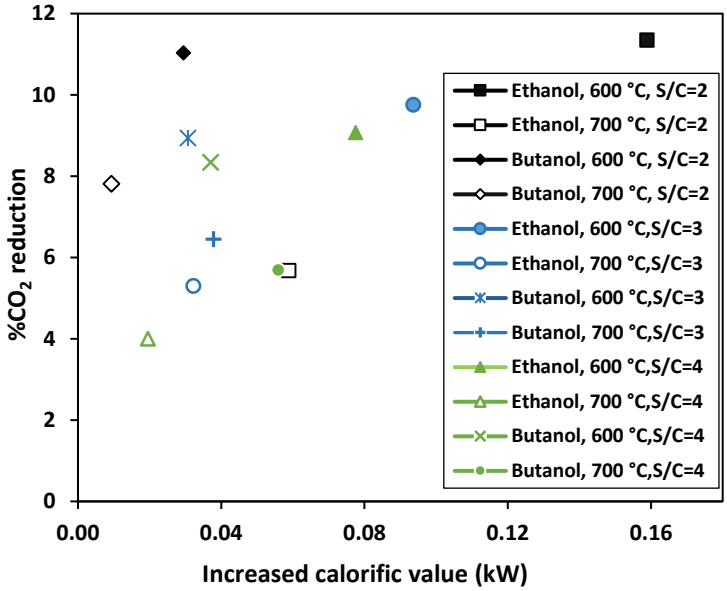

Figure 12. Increased calorific value of the reformate and CO2 reduction rate for ethanol and butanol, as a function of temperature and steam to carbon molar ratio.

As it is indicated in Figure 12, reforming reactions across the catalyst would improve calorific value of input fuel on account of dominance of endothermic reforming reactions on exothermic reactions. The results reveal that both fuels provide significant boost in calorific value of the reformer feed fuel which is a function of S/C ratio and reforming temperature.

At a constant reformer inlet temperature of 600 °C, reforming reactions increase baseline fuel calorific value in the range of 0.08-0.16 kW and 0.03-0.04 kW for ethanol and butanol, respectively. Counterpart calorific value increments at 700 °C are 0.02-0.06 kW for ethanol and 0.01-0.06 kW for butanol. Among the two fuels, at lower temperature, ethanol presents higher efficiency, about 130% at temperature 600 °C and S/C of 4.0, resulting in higher maximum increased calorific value compared

to butanol. However, at higher catalyst inlet temperature and S/C ratio, butanol reforming generally presents more efficient behaviour compared to ethanol.

Figure 13 shows that ethanol and butanol exhaust gas fuel reforming can provide a significant energy replacement and subsequently noticeable fuel saving under studied steam to carbon ratios and temperatures. The energy replacement results for both fuels are consistent with the trends demonstrated in Figure 5. Considering ethanol results at 600 °C, firstly, the peak energy replacement happens at steam to carbon ratio of 2.0, where H_2 production from ethanol reforming is on its maximum level. This trend is then followed by a gradual drop at 700 °C for all tested steam to carbon ratios, similar to H_2 production rate in Figure 5 (b). Meanwhile results reveal that butanol energy replacement level increases particularly by temperature when operating condition is more favourable for efficient butanol fuel reforming, as shown in Figure 5 (a).

Figure 13 shows that with reducing fuel flow rate entering the reforming catalyst (increasing S/C) the energy replacement level decreases in every instance. As a result, some of the additional fuel is consumed by endothermic fuel reforming reactions (steam and dry reforming) leading to additional H_2 rate supply to the engine intake. This results in reformate enthalpy enhancement and fuel economy improvement. This is clearly indicated in Figure 5 (b) and Figure 8 (b) for ethanol at 700 °C conditions. In this case raising fuel injection rate (reducing S/C), increases the H_2 and CO production rates from 7.7% to 13.4%, and from 0.03% to 0.07%, respectively. These variations are enough to raise reformate enthalpy and thus energy replacement rates.

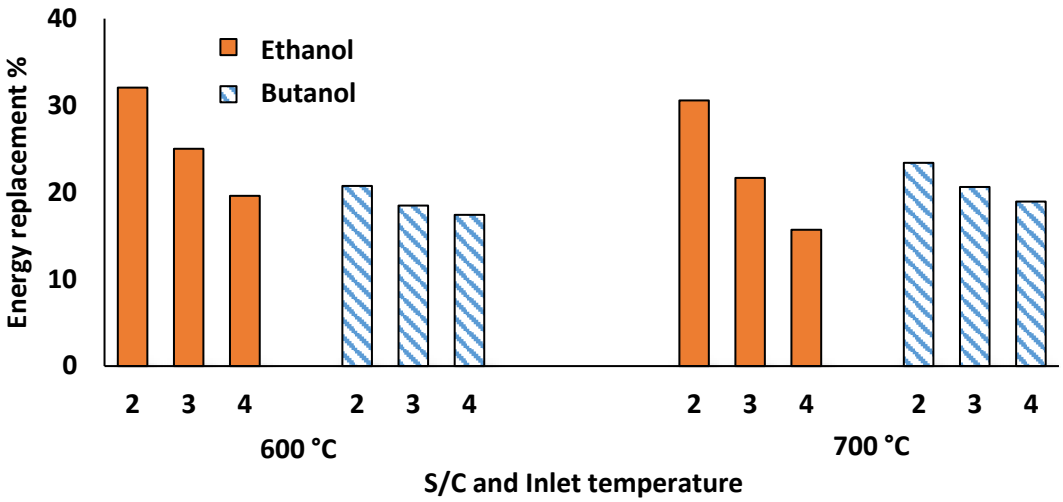

Figure 13 Energy replacement rate for ethanol and butanol, as a function of temperature and steam to carbon molar ratio.

4 Conclusion

This study is focused on catalytic reforming of renewable fuels using exhaust thermochemical recovery for gasoline direct injection engine technology under lean operation. Experimental and thermodynamic study was carried out to investigate the conversion of pure renewable fuels toward H_2 production in a fixed bed reactor on a Rh/CZA coated catalyst. Furthermore, the additional benefits of using the fuels, as reformed fuels, such as improvement in exhaust heat recovery, fuel economy and CO_2 reduction are understood as a function of steam to carbon molar ratio and catalyst inlet temperature. The main conclusions of experimental and thermodynamic equilibrium analysis of ethanol and butanol fuel reforming are as the following:

- High H_2 production and complete fuel conversion, especially at high catalyst inlet temperature, justify the promising stability and activity of Rh/CZA catalyst under different reaction conditions. Also, there is no evidence for coke formation and carbon poisoning on the utilised catalyst.
- The overall results indicate that, at higher inlet temperatures, for both fuels, reforming process is mainly endothermic being controlled by steam and dry reforming reactions.
- At lower catalyst inlet temperatures, ethanol fuel reforming process generates more H_2, while butanol presents a better performance in terms of engine fuel economy, energy replacement

by reformate, and CO_2 reduction at higher temperature consistent with ascending process efficiency.

- In terms of fuel replacement competence, butanol needs higher temperature than ethanol to offer comparable H_2 production and fuel conversion efficiency. In this case, the maximum process efficiency of ~ 130% can be obtained at 700 °C and steam to carbon ratio of 4.0.
- Maximum heating value increment of 0.16 kW, corresponding to 0.28 kW input fuel, maximum energy replacement 32.1% and CO_2 reduction of 11.4% are obtained by ethanol fuel reforming at 600 °C and steam to carbon ratio of 2.0. While at higher reforming temperature, 700 °C, butanol fuel reforming is more advantageous resulting in 27% further CO_2 reduction and higher heating value increment compared to ethanol.

The main limitation of this study are listed as the following:

- There is no known developed surface mechanism for this specific fuel reforming catalyst (Rh/CZN), therefore the equilibrium calculations will diverge from experimental results.
- The engine fuel replacement and CO_2 reduction by reformate was estimated assuming unchanged engine thermal efficiency and combustion efficiency. However, in reality, both thermal efficiency and combustion efficiency will change and there will be some differences in these estimations.
- Catalyst durability/stability and thermal deactivation of the catalyst are not investigated at high reforming temperature.
- Interaction between engine and reformer is complicated as reformate composition is highly dependent on reformer operating condition, including catalyst inlet temperature, flow rate and reactant composition and the variation of the reformate composition will affect engine performance.

Finally, it is demonstrated that promising fuel replacement and, subsequently, thermochemical recovery, fuel saving, and emission reduction are achievable by operating under specific conditions for each fuel, as reported in the study.

The potential of renewable fuel reforming in exhaust thermochemical recovery deserves further studies to provide more insight into the benefits and challenges when the reformate gas is recirculated back to the engine. Those further studies will contribute towards the effective implementation of this approach in practical and full-scale applications.

Acknowledgments

Moloud Mardani would like to thank University of Birmingham for her scholarship. EPSRC (EP/P03117X/1) is acknowledged for supporting this work and Johnson Matthey for providing the catalysts.

References

[1] Granovskii M, Dincer I and Rosen M A 2007 Exergetic life cycle assessment of hydrogen production from renewables *J. Power Sources* **167** 461–71

[2] Agudelo A F, García-Contreras R, Agudelo J R and Armas O 2016 Potential for exhaust gas energy recovery in a diesel passenger car under European driving cycle *Appl. Energy* **174** 201–12

[3] Saidur R, Rezaei M, Muzammil W K, Hassan M H, Paria S and Hasanuzzaman M 2012 Technologies to recover exhaust heat from internal combustion engines *Renew. Sustain. Energy Rev.* **16** 5649–59

[4] Tsolakis A, Megaritis A and Wyszynski M L 2003 Application of Exhaust Gas Fuel Reforming in Compression Ignition Engines Fueled by Diesel and Biodiesel Fuel Mixtures *Energy & Fuels* **17** 1464–73

[5] Tartakovsky L, Baibikov V, Gutman M, Poran A and Veinblat M 2014 Thermo-Chemical Recuperation as an Efficient Way of Engine's Waste Heat Recovery *Appl. Mech. Mater.* **659** 256–61

[6] Gaber C, Demuth M, Schluckner C and Hochenauer C 2019 Thermochemical analysis and experimental investigation of a recuperative waste heat recovery system for the tri-reforming of light oil *Energy Convers. Manag.* **195** 302–12

[7] Pashchenko D 2020 Thermochemical waste-heat recuperation as on-board hydrogen production technology *Int. J. Hydrogen Energy*

[8] Pashchenko D, Gnutikova M and Karpilov I 2020 Comparison study of thermochemical waste-heat recuperation by steam reforming of liquid biofuels *Int. J. Hydrogen Energy* **45** 4174–81

[9] Tartakovsky L and Sheintuch M 2018 Fuel reforming in internal combustion engines *Prog. Energy Combust. Sci.* **67** 88–114

[10] Fennell D, Herreros J and Tsolakis A 2014 Improving gasoline direct injection (GDI) engine efficiency and emissions with hydrogen from exhaust gas fuel reforming *Int. J. Hydrogen Energy* **39** 5153–62

[11] Fennell D, Herreros Arellano J M, Tsolakis A, Wyszynski M, Cockle K, Pignon J and Millington P 2017 On-board thermochemical energy recovery technology for low carbon clean gasoline direct injection engine powered vehicles *Proc. Inst. Mech. Eng. Part D J. Automob. Eng.* **232** 1079–91

[12] Bogarra M, Herreros J M, Tsolakis A, York A P E and Millington P J 2016 Study of particulate matter and gaseous emissions in gasoline direct injection engine using on-board exhaust gas fuel reforming *Appl. Energy* **180** 245–55

[13] Ashida K, Maeda H, Araki T, Hoshino M, Hiraya K, Izumi T and Yasuoka M 2015 Study of an On-board Fuel Reformer and Hydrogen-Added EGR Combustion in a Gasoline Engine *SAE Int. J. Fuels Lubr.* **8** 358–66

[14] Wang S, Ji C, Zhang M and Zhang B 2010 Reducing the idle speed of a spark-ignited gasoline engine with hydrogen addition *Int. J. Hydrogen Energy* **35** 10580–8

[15] Du Y, Yu X, Liu L, Li R, Zuo X and Sun Y 2017 Effect of addition of hydrogen and exhaust gas recirculation on characteristics of hydrogen gasoline engine *Int. J. Hydrogen Energy* **42** 8288–98

[16] Naruke M, Morie K, Sakaida S, Tanaka K and Konno M 2019 Effects of hydrogen addition on engine

performance in a spark ignition engine with a high compression ratio under lean burn conditions *Int. J. Hydrogen Energy* **44** 15565–74
[17] Steinfeld A 2002 Solar hydrogen production via a two-step water-splitting thermochemical cycle based on Zn/ZnO redox reactions *Int. J. Hydrogen Energy* **27** 611–9
[18] Turn S, Kinoshita C, Zhang Z, Ishimura D and Zhou J 1998 An experimental investigation of hydrogen production from biomass gasification *Int. J. Hydrogen Energy* **23** 641–8
[19] Jamal Y and Wyszynski M L 1994 On-board generation of hydrogen-rich gaseous fuels—a review *Int. J. Hydrogen Energy* **19** 557–72
[20] Tsolakis A, Megaritis A and Wyszynski M . 2004 Low temperature exhaust gas fuel reforming of diesel fuel *Fuel* **83** 1837–45
[21] Fennell D, Herreros J, Tsolakis A, Cockle K, Pignon J and Millington P 2015 Thermochemical recovery technology for improved modern engine fuel economy-part 1: Analysis of a prototype exhaust gas fuel reformer *RSC Adv.* **5** 35252–61
[22] Leung P, Tsolakis A, Rodríguez-Fernández J and Golunski S 2010 Raising the fuel heating value and recovering exhaust heat by on-board oxidative reforming of bioethanol *Energy Environ. Sci.* **3** 780–8
[23] Bogarra M, Herreros J M, Tsolakis A, York A P E, Millington P J and Martos F J 2017 Impact of exhaust gas fuel reforming and exhaust gas recirculation on particulate matter morphology in Gasoline Direct Injection Engine *J. Aerosol Sci.* **103** 1–14
[24] Arku P, Regmi B and Dutta A 2018 A review of catalytic partial oxidation of fossil fuels and biofuels: Recent advances in catalyst development and kinetic modelling *Chem. Eng. Res. Des.* **136** 385–402
[25] Auprêtre F, Descorme C and Duprez D 2002 Bio-ethanol catalytic steam reforming over supported metal catalysts *Catal. Commun.* **3** 263–7
[26] Chen C-C, Tseng H-H, Lin Y-L and Chen W-H 2017 Hydrogen production and carbon dioxide enrichment from ethanol steam reforming followed by water gas shift reaction *J. Clean. Prod.* **162** 1430–41
[27] Cavallaro S, Chiodo V, Vita A and Freni S 2003 Hydrogen production by auto-thermal reforming of ethanol on Rh/Al2O3 catalyst *J. Power Sources* **123** 10–6
[28] da Silva A M, de Souza K R, Jacobs G, Graham U M, Davis B H, Mattos L V. and Noronha F B 2011 Steam and CO2 reforming of ethanol over Rh/CeO2 catalyst *Appl. Catal. B Environ.* **102** 94–109
[29] Lima da Silva A, Malfatti C de F and Müller I L 2009 Thermodynamic analysis of ethanol steam reforming using Gibbs energy minimization method: A detailed study of the conditions of carbon deposition *Int. J. Hydrogen Energy*
[30] Nahar G A and Madhani S S 2010 Thermodynamics of hydrogen production by the steam reforming of butanol: Analysis of inorganic gases and light hydrocarbons *Int. J. Hydrogen Energy* **35** 98–109
[31] Marchal R, Ropars M, Pourquié J, Fayolle F and Vandecasteele J P 1992 Large-scale enzymatic hydrolysis of agricultural lignocellulosic biomass. Part 2: Conversion into acetone-butanol *Bioresour. Technol.* **42** 205–17
[32] Bîldea C S, Patraşcu I, Segovia Hernandez J G and Kiss A A 2016 Enhanced Down-Stream Processing of Biobutanol in the ABE Fermentation Process *Comput. Aided Chem. Eng.* **38** 979–84
[33] Shejale A D and Yadav G D 2019 Noble metal promoted Ni–Cu/La2O3–MgO catalyst for renewable and enhanced hydrogen production via steam reforming of bio-based n-butanol: effect of promotion with Pt, Ru and Pd on catalytic activity and selectivity *Clean Technol. Environ. Policy* **21** 1323–39
[34] Harju H, Lehtonen J and Lefferts L 2015 Steam- and autothermal-reforming of n-butanol over Rh/ZrO2 catalyst *Catal. Today* **244** 47–57
[35] Harju H, Lehtonen J and Lefferts L 2016 Steam reforming of n-butanol over Rh/ZrO2 catalyst: role of 1-butene and butyraldehyde *Appl. Catal. B Environ.* **182** 33–46
[36] Cai W, Piscina P R de la, Gabrowska K and Homs N 2013 Hydrogen production from oxidative steam reforming of bio-butanol over CoIr-based catalysts: Effect of the support *Bioresour. Technol.* **128** 467–71
[37] Cai W, Piscina P R de la and Homs N 2012 Hydrogen production from the steam reforming of bio-butanol over novel supported Co-based bimetallic catalysts *Bioresour. Technol.* **107** 482–6
[38] Bimbela F, Oliva M, Ruiz J, García L and Arauzo J 2009 Catalytic steam reforming of model compounds of biomass pyrolysis liquids in fixed bed: Acetol and n-butanol *J. Anal. Appl. Pyrolysis* **85** 204–13
[39] Lin K-W and Wu H-W 2018 Hydrogen-rich syngas production of urea blended with biobutanol by a thermodynamic analysis *Int. J. Hydrogen Energy* **43** 17562–73
[40] Horng R-F, Lai M-P, Chiu W-C and Huang W-C 2016 Thermodynamic analysis of syngas production and carbon formation on oxidative steam reforming of butanol *Int. J. Hydrogen Energy* **41** 889–96
[41] Wang W 2011 Hydrogen production via dry reforming of butanol: Thermodynamic analysis *Fuel* **90**

1681–8
[42] Kumar B, Kumar S S and Kumar S S 2017 Thermodynamic and energy analysis of renewable butanol–ethanol fuel reforming for the production of hydrogen *J. Environ. Chem. Eng.* **5** 5876–90
[43] Patel M, Jindal T K and Pant K K 2013 Kinetic Study of Steam Reforming of Ethanol on Ni-Based Ceria–Zirconia Catalyst *Ind. Eng. Chem. Res.* **52** 15763–71
[44] Yadav A K and Vaidya P D 2018 Reaction Kinetics of Steam Reforming of n-Butanol over a Ni/Hydrotalcite Catalyst *Chem. Eng. Technol.* **41** 890–6
[45] Kee R J, Rupley F M and Miller J A 1989 *Chemkin-II: A Fortran chemical kinetics package for the analysis of gas-phase chemical kinetics* (Sandia National Labs., Livermore, CA (USA))
[46] Dhanala V, Maity S K and Shee D 2015 Oxidative steam reforming of isobutanol over Ni/γ-Al2O3 catalysts: A comparison with thermodynamic equilibrium analysis *J. Ind. Eng. Chem.* **27** 153–63
[47] Katiyar N, Kumar S and Kumar S 2013 Comparative thermodynamic analysis of adsorption, membrane and adsorption-membrane hybrid reactor systems for methanol steam reforming *Int. J. Hydrogen Energy* **38** 1363–75
[48] Mehl M, Curran H J, Pitz W J and Westbrook C K 2009 *Chemical kinetic modeling of component mixtures relevant to gasoline* (Lawrence Livermore National Lab.(LLNL), Livermore, CA (United States))
[49] Sarathy S M, Vranckx S, Yasunaga K, Mehl M, Oßwald P, Metcalfe W K, Westbrook C K, Pitz W J, Kohse-Höinghaus K, Fernandes R X and Curran H J 2012 A comprehensive chemical kinetic combustion model for the four butanol isomers *Combust. Flame* **159** 2028–55
[50] Kirillov V A, Meshcheryakov V D, Sobyanin V A, Belyaev V D, Amosov Y I, Kuzin N A and Bobrin A S 2008 Bioethanol as a promising fuel for fuel cell power plants *Theor. Found. Chem. Eng.* **42** 1–11
[51] Hergueta C, Tsolakis A, Herreros J M, Bogarra M, Price E, Simmance K, York A P E and Thompsett D 2018 Impact of bio-alcohol fuels combustion on particulate matter morphology from efficient gasoline direct injection engines *Appl. Energy* **230** 794–802
[52] Villegas L, Guilhaume N, Provendier H, Daniel C, Masset F and Mirodatos C 2005 A combined thermodynamic/experimental study for the optimisation of hydrogen production by catalytic reforming of isooctane *Appl. Catal. A Gen.* **281** 75–83
[53] López Ortiz A, Pallares Sámano R B, Meléndez Zaragoza M J and Collins-Martínez V 2015 Thermodynamic analysis and process simulation for the H2 production by dry reforming of ethanol with CaCO3 *International Journal of Hydrogen Energy* vol 40 (Elsevier Ltd) pp 17172–9
[54] Hartley U W, Amornraksa S, Kim-Lohsoontorn P and Laosiripojana N 2015 Thermodynamic analysis and experimental study of hydrogen production from oxidative reforming of n-butanol *Chem. Eng. J.* **278** 2–12
[55] Kumar B, Kumar S and Kumar S 2018 Thermodynamic analysis of H 2 production by oxidative steam reforming of butanol-ethanol-water mixture recovered from Acetone:Butanol:Ethanol fermentation *Int. J. Hydrogen Energy*
[56] Wang W and Cao Y 2011 Hydrogen production via sorption enhanced steam reforming of butanol: Thermodynamic analysis *Int. J. Hydrogen Energy*
[57] Ahmed S and Krumpelt M 2001 Hydrogen from hydrocarbon fuels for fuel cells *Int. J. Hydrogen Energy* **26** 291–301